PROTECTIVE POTENTIALS OF Moringa oliefera-MEDIATED IRON OXIDE NANOPARTICLES AGAINST MERCURY INDUCED OXIDATIVE STRESS AND BAX GENE mRNA EXPRESSION IN RATS

Nwobegu J. S, Odeleye A. A, and Onifade I. L
Department of Science Technology, The Federal Polytechnic Ado-Ekiti, Ekiti State Nigeria
e-mail: snwobegu@gmail.com. phone no. 08038690519

Abstract
This study investigates the Protective potentials of Moringa olifera-mediated iron nanoparticles against mercury-induced oxidative stress and BAX gene mRNA expression in rats. Moringa oleifera leaves (MOL) were obtained from Ado-Ekiti and authenticated by a Botanist. Dried and powder leave was extracted in ratio 1:1 absolute ethanol/deionized. The green synthesis of moringa olifera iron oxide nanoparticles (MOLE-FeONPs) was done using a bottom-up process approach. The UV–visible spectra was used to monitor the synthesis, while characterization was done using SEM, EDX, XRD and FTIR, respectively. Forty male rats of comparable weight and age were used for the experiments. The animals were randomly allocated into eight groups of five rats each and administered orally in the following ways: Group I: control rats received normal saline. Group II: Rats received MOLE. Group III: Rats received FeNPs. Group IV: Rats received MOLE-FeNPs. Group V: Rats received mercury. Group VI: Rats received Hg + MOLE. Group VII: Rats received Hg + FeNPs. Group VIII: Rats received Hg + MOLE-FeNP. The animals were sacrificed after 21 days, blood, Kidney, Liver, and Testis tissues were collected for further analyses. Result showed that increase in MDA (6.86 ± 0-49 -2.61 ± 0.28) and LDH (189.32 ± 10.86 -57.49 ± 6.56) in rat's kidney were ameliorated by green synthesized MOLE-FeNPs. The activities SOD(0.76 ± 0.08 – 2.05± 0.3), CAT(3.81 ±,0.2 – 6.42 ± 0.4), GSH(0.05 ± 0.02 – 0.24 ± 0.01), GPx(64.10 ± 2.96 – 78.82 ± 5.60, and TAC(0.64± 0.02 – 0.77 ± 0.05) significantly increased with the administration of MOLE-FeNP respectively. The transcriptional levels of apoptosis-related gene (Bax), was ameliorated when treated with MOLE-FeNP from 4.3 -1.8µm. Therefore MOLE- FeNPs has protective prospect against mercury induced oxidative stress and expression of apoptosis related genes in rats.

1.0 INTRODUCTION

Nanoparticles are extremely small particles, ranging in size from 1 to 100 nm. Based on their characteristics, forms, or sizes, they can be divided into many classifications. Fullerenes, metal NPs, ceramic NPs, and polymeric NPs are some of the many groupings. Due to their large surface area and nanoscale size, NPs have distinct physical and chemical characteristics. According to reports, the size influences their optical characteristics and imparts various hues through visible-range absorption. They make good candidates for a variety of industrial and household uses, including as catalysis, imaging, medicinal applications, energy-based research, and environmental applications. Mercury (Hg), is a heavy metal with an atomic weight of 200.6 g mol1, a density of 13.6 and special properties. At room temperature, it is the only metal that is liquid. Additionally, it may be found in nature in three different forms: organic, inorganic, and elemental. Elemental mercury vapor makes up the majority of mercury in the atmosphere, whereas organic and inorganic species prevail in soil, water, plants, and animals. Methyl mercury, an organic form of mercury, is created when microorganisms in soil and water methylate inorganic forms of mercury (Castoldi et al., 2003). Because mercury and the majority of its compounds are so dangerous, they must be handled carefully. Among the harmful effects are damage to the brain, kidneys, and lungs. Acrodynia (also known as "pink disease"), Hunter-Russell syndrome, and Minamata disease are only a few of the illnesses that can be brought on by mercury exposure (Hammond, 2008). About 40% of the population reported using medicinal plants for therapeutic purposes, and the usage of herbal medicines is increasing (Ekor, 2014). The Moringa oleifera (MO), a member of the Moringaceae family, is known as "The Miracle Tree" and is grown in many nations throughout the world (Bhattacharya et al., 2018). It has been utilized for millennia due to its beneficial nutritional and health-promoting features around the world (Vergara-Jimenez et al., 2017). The medicinal properties of MO include hepato-protective, neuro-protective,

antioxidant, anti-inflammatory, anti-carcinogenic, antimicrobial, and immune-improving activities (Abd-Elhakim et al., 2018; El-Hadary and Ramadan, 2019; El Shanawany et al., 2019; Obembe and Raji,(20). MO also produce significant amounts of saponins, tannins, flavonoids, glycosides, In Mansour et al.'s (2014) study, renal effects of MO against heavy metal protection by controlling renal functions, preventing oxidative damage, and reducing inflammatory responses, Mansour et al. (2014) showed that MO has renal protective effects against heavy metal poisoning. A number of chronic illnesses are also prevented or treated with MOLE. According to studies by Abou-Zeid et al., (2020), Khalil et al., (2020), and Mansour et al., (2020), MOLE is effective in protecting against tilmicosin-induced nephrotoxicity, cardiac toxicity in rats, and reproductive toxicity. The antibacterial, anti-inflammatory, anti-cancer, and anti-diabetic properties of moringa oliefera leaves (MOL) have been briefly investigated (Anwar et al., 2007). Minerals, vitamins, carotenoids, phenolic acids, and flavonoids were classified in MOLE and are associated with MOLE-enhanced antioxidant effects (Karthivashan et al., 2015). The polyphenol concentration of MOLE has high anti-oxidant properties that mitigate the effects of free radicals and oxidative stress (OS) (Sreelatha and Padma, 2009). Aja et al. (2014) concluded that methanolic MOLE contains chemical constituents not found in MO seeds. The evolvement of green and sustainable methods for nanoparticles synthesis has been a recent research focus (Adil *et. al*., 2015). Frequently, plant extracts are effective precursors for the production of metallic nanoparticles (Khan *et. al.,* 2018). Iron nanoparticles (FeNPs) are sub-micrometer particles of iron metal. They are highly reactive because of their large surface area. In the presence of oxygen and water, they rapidly oxidize to form free iron ions and they are non – toxic. FeNPs, are frequently synthesized using various plants, such as green tea (Shahwan *et. al.,* 2011), Sorghun sp (hybrid sorghum) (Njagi *et. al.,*2011), Eucalyptus globulus (Madhavi *et. al.,* 2013), plantain peel (Venkates warlu *et. al.,* 2013), Grape seed proanthrocynidin (Narayanan *et. al.,*2012) However, to the best of our knowledge, there have been no prior studies of MOLE-FeO-NPs or MOLE on Mercury-induced oxidative stress and Bax mRNA gene expression. Numerous studies have shown how effective natural products are in reducing the toxic effects of Mercury. The primary goal of the current study was to create and characterize green FeO-NPs using an ethanolic M. oleifera leaf extract (MOLE-FeO-NPs). Second, the study compared, for the first time, the in vivo protective effects of MOLE-FeO-NPs conjugate or MOLE as treatments for Mercury-induced oxidative stress and Bax mRNA gene expression in male rats.

2.0 MATERIALS AND METHODS

2.1 Chemicals

Assays were done using standard ELISA kits. All other reagents used, unless otherwise indicated, were of analytical grade. Iron (III) chloride hexahydrate ($FeCl_3.6H_2O$) and sodium hydroxide (NaOH) pellets were purchased from a chemical shop in Nigeria. The chemicals were further used without any purification.

2.2 Plant extract preparation *Moringaoleifera*leaves extract(MOLE)

Moringa oleifera leaves (MOL) were obtained from Ado-Ekiti and authenticated by a Botanist. Dried *M. oleifera* leaves were crushed into a powder using a high-speed milling device. One thousand grams of powder was extracted in ratio 1:1 absolute ethanol/ deionized water for 48 hours then filtered twice through filter paper with 2 µm pore size. The resultant extract was concentrated and evaporated to dryness using a rotary evaporator at 40–45 °C. The residual yield of MOLE extract was 63.8 g/1000 g of dried sample was obtained. The obtained extract was kept at 4°C until use. Both *M. oleifera* leaves and the extract were subjected to phytochemical screening following the standard procedure to identify the presence of active constituents such as flavonoid, tannin, glycoside, alkaloids, saponin, steroids, and phenol.

2. 3 Synthesis of Iron Nanoparticle (FeNPs)

Iron Nanoparticles (FeNPs) was synthesized by adding 0.1M Iron (III) chloride hexahydrate ($FeCl_3.6H_2O$) to 0.2M Iron (IV) sulphate ($FeSO_4.7H_2O$) and stirred. Ammonium Hydroxide solution was added dropwise until colour change to dark brown solution to confirm the synthesis of FeO-NPs. The synthesized FeO-NPs were separated by centrifugation for 15 min and the pellet containing FeO-NPs were washed (3 times) with deionized water followed by drying at 80 °C for 3 h and stored for further use.

2. 4 Synthesis of MOLE based Iron Nanoparticle (MOLE-FeO-NPs)

The green synthesis of iron oxide (Fe_2O_3) nanoparticles using plant extract was performed by a bottom-up process approach and reduction technique by a single pot system revamping the procedure by Chatterjee *et al.* (2021). 100 mL of 3 mM of $FeCl_3.6H_2O$ was added to a beaker. Then 10ml of the plant extract was added to 90ml of deionized water. The mixture was slowly added into $FeCl_3$ solution and was allowed to react. The solution was adjusted to pH 11 by adding 1 M NaOH, and the mixture stirred continuously for 2 h. The formation of a dark brown colour solution confirmed the synthesis of MOLE-FeNPs. Nanoparticles formation was further confirmed using UV–visible spectra of a Mobi Microplate spectrophotometer. The synthesized MOLE-FeO-NPs were separated by centrifugation at 12,000×*g* for 15 min and the pellet containing MOLE- FeO-NPs were washed (3 times) with deionized water followed by drying at 60 °C for 1 h and stored for further use.

2. 5 Characterization of MOLE-FeNPs

The morphology, shape, size and purity of the nanoparticles were analyzed by a scanning electron microscope (SEM) [Tecnai G2 spirit Biotwin (FP 5018/40), operating at around 80 kV accelerating voltage] and a scanning electron microscope (SEM) (Hitachi S 3400 N) outfitted with an Energy Dispersive X-ray Spectroscopy (EDX), respectively. The zeta potential (Charge distribution) of the nanoparticles was studied using a Beckman Coulter DelsaTM Nano Particle Analyzer (USA) by illuminating the solution with a He–Ne laser (658 nm) in a sample cell. The crystallinity of the FeO-NPs was analysed by XRD. The diffracto gram was documented by PANalytical, XPERTPRO diffractometer using Cuk (Cu Kα radiation, λ 1.54443) as X-ray source running at 45 kV and 30 mA. Fourier transform infrared spectroscopy (FTIR, Shimadzu 8400 S) was employed to functional groups, present in synthesized FeO-NPs.

2. 6 Experimental animals

Forty male rats of comparable weight and age (10±2 weeks, 200±20g) housed in standard well-ventilated cages (maximum of 5 animals/cage), in the Animal Holdings of the Department of Science Technology, The Federal Polytechnic Ado-Ekiti, Nigeria. The rats were provided with standard chow and water *ad libitum* and subjected to the natural photoperiod of 12 h light/dark cycle with room temperature 25 ± 2ºC and humidity 60 ± 5%. All animals were cared for humanely according to the conditions stated in the Guide for the Care and Use of Laboratory Animals' of the National Academy of Science (NAS), published by the National Institute of Health. The study also followed National Institutes of Health's recommendations for the care and use of laboratory animals, and adequate procedures were made to ensure that the animals were not subjected to excessive pain and discomfort during the study.

2.7.0 Experimental procedure

Animals were randomly allocated into eight groups of five rats each and administered orally in the following ways:

Group I: control rats received 1mL of 0.9% normal saline. Group II: rats received MOLE (800 mg/kg BW). Group III: rats received FeNPs (250 µg//kg BW). Group IV: rats received MOLE-FeNPs (200 µg//kg BW). Group V: rats received mercury (0.5 mg/kg BW). Group VI: rats received Hg (0.5 mg/kg BW) + MOLE (800 mg/kg BW). Group VII: rats received Hg (0.5 mg/kg BW) + FeNPs (250 µg/kg BW).Group VIII: rats received Hg (0.5 mg/kg BW) + MOLE-FeNP (200 µg/kg BW).

Gavage was day after day for 28 days, using a feeding needle. All animals were carefully observed throughout the experiment for any signs of intoxication or mortalities.

2.7.1 Blood and tissue sample collection

Twenty-four hours after the last treatment, the over-night-fasted rats were weighed and anesthetized with ketamin at the end of the dosing period. Two mL blood samples were collected from the rats via cardiac puncture. Blood was collected using a BD Vacutainer PST II Tubes, left for coagulation, then centrifuged at 322 x g for 20 min for serum separation. Sera were preserved at– 20 °C until biochemical analysis.

Kidney, liver and testis tissues were collected and divided into four portions.

Thirty mg was washed in cold saline and mix with RNA shield for storage before RNA extraction. For RT-PCR analysis of apoptosis and stress related Bcl -2 Associated X-protien (Bax) gene expression,,

the remaining portion stored for mercury analysis.

2.7.2 Serum and tissue mercury analysis

One mL/mg of serum/tissues were digested with 10 mL analytical grade H_2O_2 (hydrogen peroxide)

and HNO_3 (nitric acid) (1:1) in a Teflon beaker. The solution was then made up to 25 mL with distilled water. Hg concentration in samples were analysed with thermal decomposition couped atomic absorption spectrophotometry (AAS) (Santos *et al.*, 2020). All analysis were investigated in triplicate.

2.7. 3 Oxidative stress biomarkers analyses

Serum sample was used to evaluate the activities of superoxide dismutase (SOD), glutathione peroxidase (GPx), Malondialdehyde (MDA), catalase (CAT), Lactic acid dehydrogenase (LDH), Total antioxidant capacity (TAC) and the concentrations of glutathione (GSH) using the analysis kits as described by the manufacturer (Nanjing Jiancheng Bioengineering Institute, Nanjing, China). All analysis was performed with Mobi Microplate spectrophotometer (Sunnyvale, CA).

3. 0 RESULTS

All experimental groups showed no altered clinical observations or behavioral alterations except for Hg-exposed rats displayed a decreased activity, food consumption, and body weights with frequently increased urination when compared with the other experimental groups. Meanwhile, rats from the Hg-MOLE, Hg-FeNP and Hg-MOLE-FeNP groups were clinically normal and did not exhibit any signs of toxicity.

3.1 Characterization of green synthesized FeO-NPs

3.1.1 UV–visible spectroscopic analysis of FeO-NPs

FeNPs were synthesized by reduction of Fe into FeNPs after the addition of MOLE filtrate and stirring for 1 h at 60°C. The stimulation of the surface plasmon resonance of FeO-NPs gave the reaction solution its distinctive brown-red colour, which served as a useful spectroscopic hallmark of their production (Fig. 1). In the identical experimental circumstances, neither the positive control group ($FeCl_3$ Solution) nor the negative control group (MOLE) showed any significant colour change. Using a UV–Visible spectrophotometer, the reduction of ferric oxide was analysed spectroscopically. This revealed a 270 nm absorbance peak (Figure 2), which was unique to FeO-NPs

3.1.2 *FTIR analysis of FeO-NPs*

The FTIR spectra of the green synthesized FeO-NPs highlighted the functional groups present in FeO-NP (Figure 3). The peak that appeared near 660 cm^{-1} could be assigned to the stretching vibration of the Fe–O–Fe bond in FeO-NPs (Rahman *et al.,* 2011). The peaks found in between 3400 and 3300 cm^{-1}, 1630 cm^{-1}, 1400 cm^{-1} and 1057 cm^{-1} were assigned to stretching vibration of O–H bond, stretching vibration C═O bond, bending vibration of C–H and stretching vibration of C–N bond, respectively (Karade *et al.*, 2019). The occurrence of these bonds can be attributed to the presence of the phenolic hydroxyl group, phenolic acids, terpenoids-phenols, and aliphatic amines. These functional groups are also responsible for the reduction of Fe^{3+} ions and behave as the capping agent of the nanoparticles (Karade *et al.,* 2019).

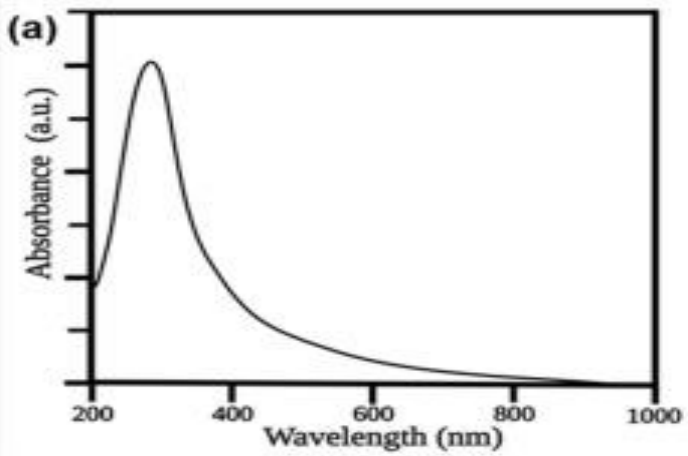

figure 2

Figure 1. Three conical flasks containing (a) only Moringa oliefera leave Extract (MOLE), (b) the reaction mixture of MOLLE and $FeCl_3$ solution, (c) only $Fecl_3$ solution, respectively. Figure2. UV-Spectroscopy

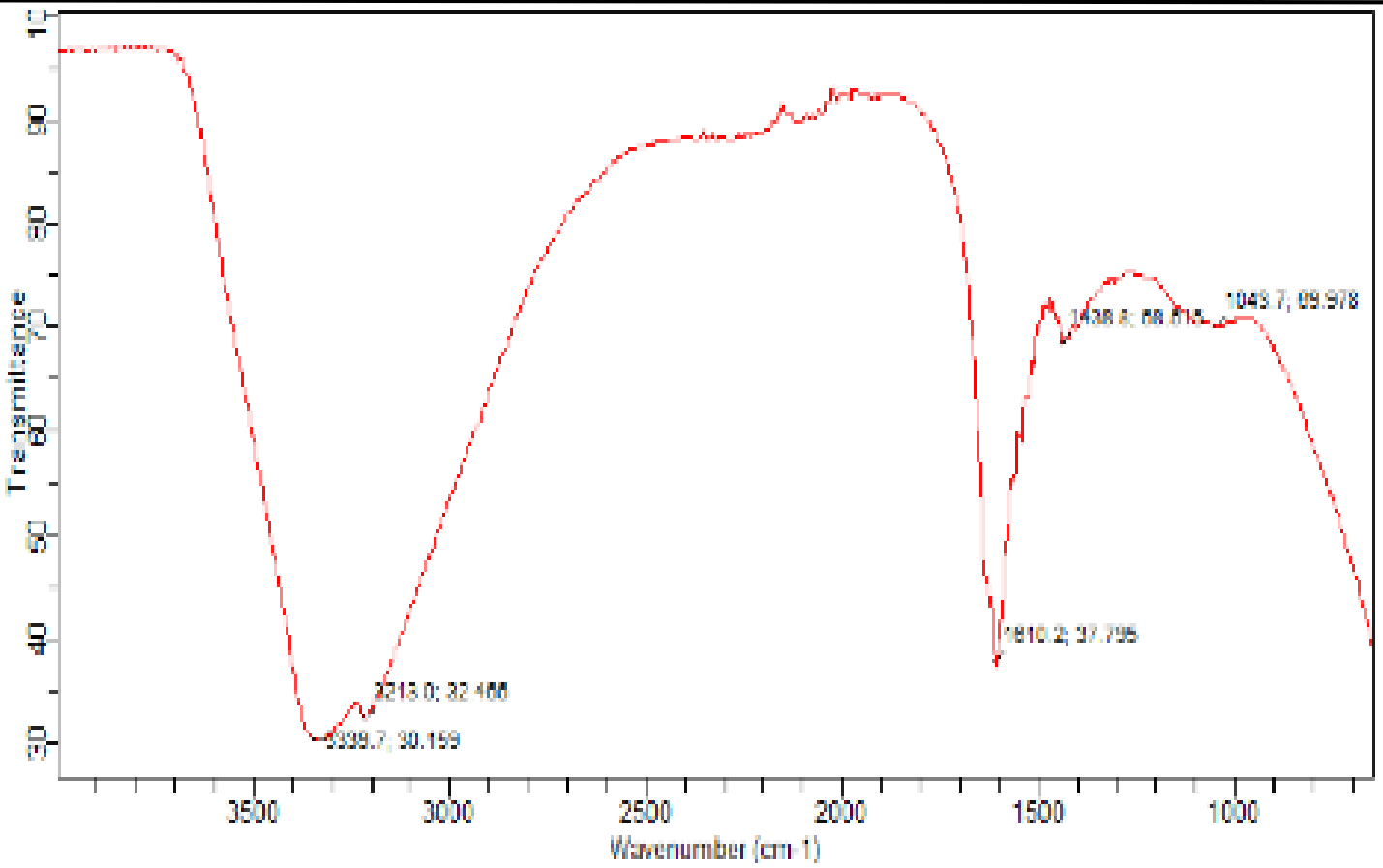

Fig.3. The FTIR spectra of FeO-NP

3.1.3 *XRD study of IONPs*

The XRD measurement is frequently found to be a valuable analytical tool for determining the crystalline nature of freshly generated compounds and their phases. The XRD pattern of the FeO-NPs, shown in Figure 4, clearly identified the fcc structure of α-Fe_2O_3 nanoparticles (JCPDS file, No. 89–2810) . During this measurement, a sequence of diffraction peaks was detected that were consistent with the theory. The prominent peaks of the XRD pattern suggest that the green synthesized FeO-NPs were well-crystallized *α*-Fe_2O_3.

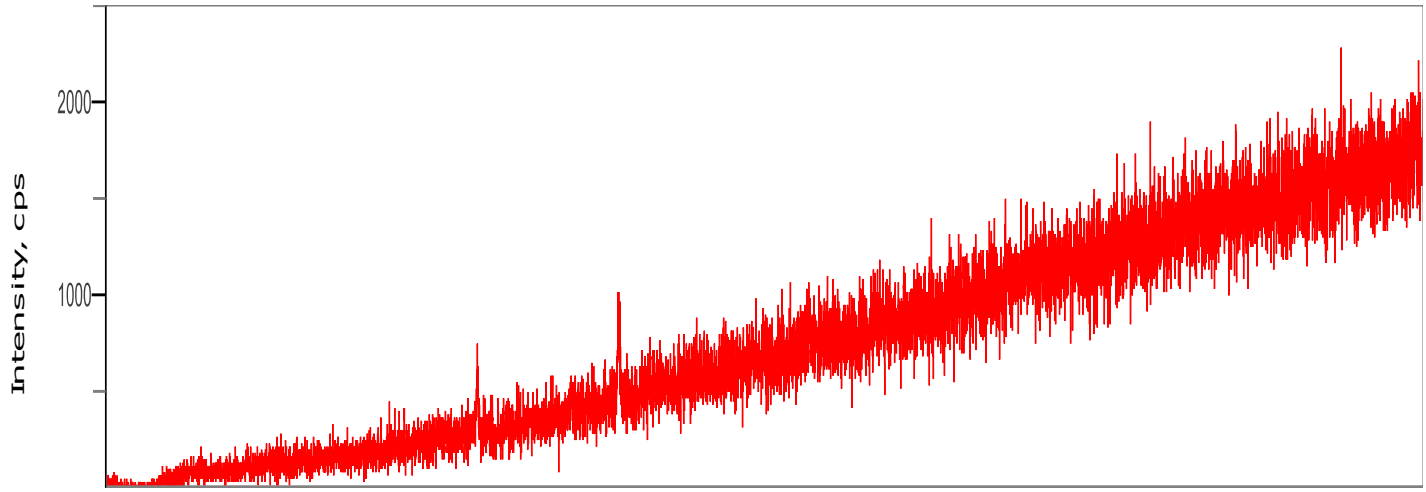

Fig. 4. XRD pattern of green synthesized FeO-NPs.

3.1.4 *EDX observation of FeO-NPs*

The EDX spectrum from one of the densely populated ferric oxide nanoparticles regions, obtained in the spot-profile mode, showed two distinct signals of iron (Fe) and oxygen (O) in synthesized FeO-NPs. Peak related to any other element did not appear in the EDX spectrum, which confirmed that the synthesized FeO-NPs were made of Fe and O.

A Scanning Electron Microscopy (SEM) study was carried out to analyse the size and morphology of the synthesized FeO-NPs. The

average size of these FeO-NPs was 5 ± 1 nm (Range: 3–10 nm) (Figure 6). In nature, particles were found to be quasi-spherical and mono-disperse.

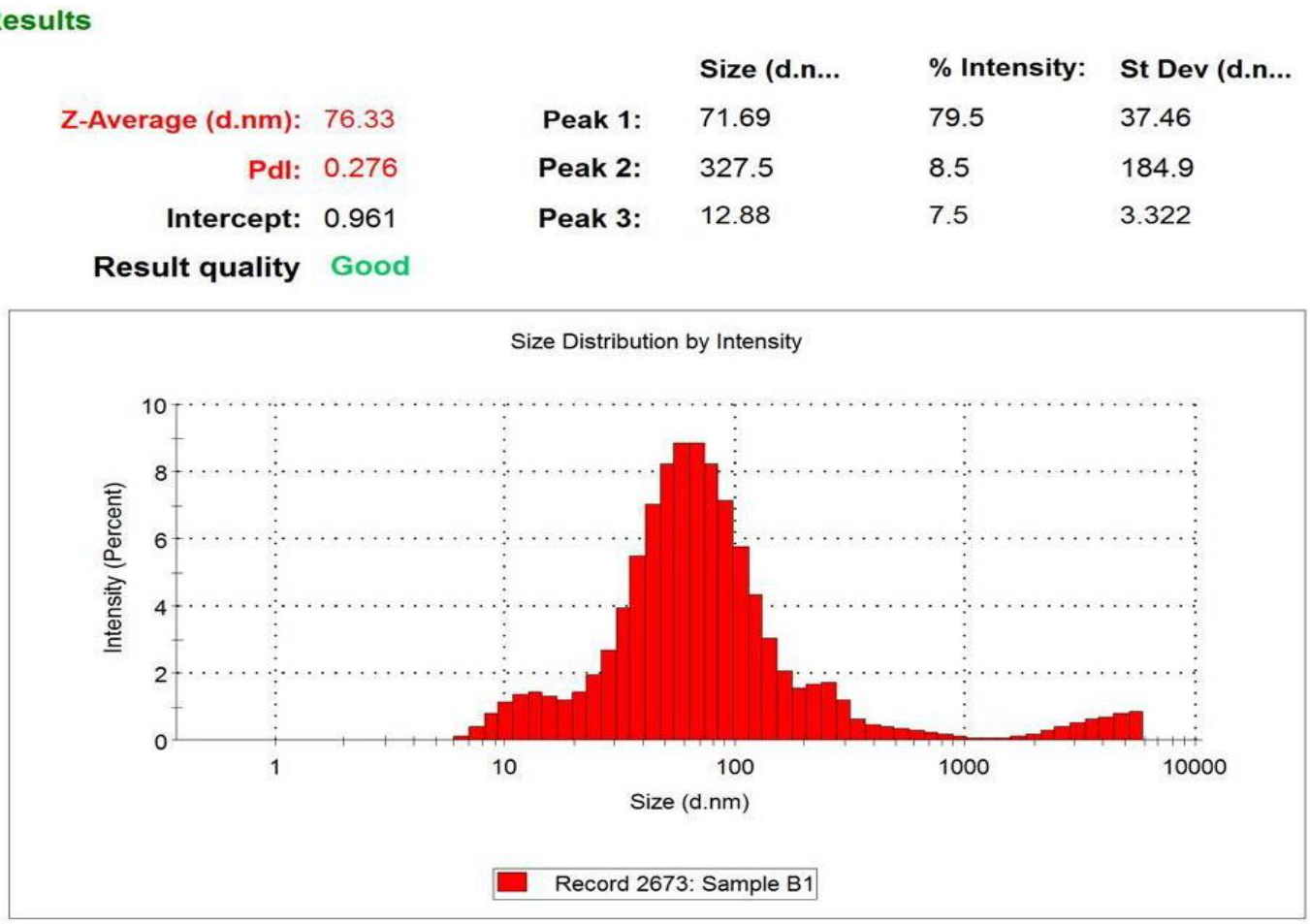

Fig. 6. Particle size of green synthesized FeO-NPs.

3.2 Relative mRNA levels of apoptosis-related genes (Bax) in renal tissues

The probability of Hg-induced renal cell apoptosis was investigated via measuring the transcriptional levels of apoptosis-related genes Bax, data are shown in (Figure 10). Hg induced increase in the expression of apoptosis related gene. However, administration of MOLE, FeNP and MOLE-FeNP ameliorates the toxic effect. The amelioration was pronounced in those that received MOLE-FeNP.

Figure 7, shows the Hg concentration in the kidney tissue. Hg was not detected in serum and tissue in control, MOLE, FeNP and MOLE-FeNP groups. However Hg concentration increased with the administration of Hg in the kidney, serum, and liver. (figures 7, 8, and 9) respectively. However, with the administration of Hg-MOLE, Hg-FeNP and Hg-MOLE-FeNP the effect of Hg reduced significantly, with Hg-MOLE-FeNPs showing most significant reduction.

3.3 Oxidative stress biomarkers

Hg-MOLE, Hg-FeNP and Hg-MOLE-FeNP conjugate impact on Hg-induced changes in oxidative stress biomarkers in male rat serum and kidney homogenates are shown in Table 1. below. There was significant increase in activities of MDA and LDH. However, this was ameliorated by Hg-MOLE-FeNP conjugate, MDA (6.86 ± 0-49 -2.61 ± 0.28) and LDH (189.32 ± 10.86 -57.49 ± 6.56) in rat's kidney.. The activities of SOD CAT, GSH, GPx. and TAC respectively in rats that were exposed to Hg were drastically reduced. Administration of Hg-MOLE, Hg-FeNP and Hg-MOLE-FeNP conjugate, increased their activities SOD(0.76 ± 0.08 – 2.05± 0.3), CAT(3.81 ±,0.2 – 6.42 ± 0.4), GSH(0.05 ± 0.02 – 0.24 ± 0.01), GPx(64.10 ± 2.96 – 78.82 ± 5.60, and TAC(0.64± 0.02 – 0.77 ± 0.05) significantly with MOLE-FeNP having the greatest impact. as shown in table 1 below.

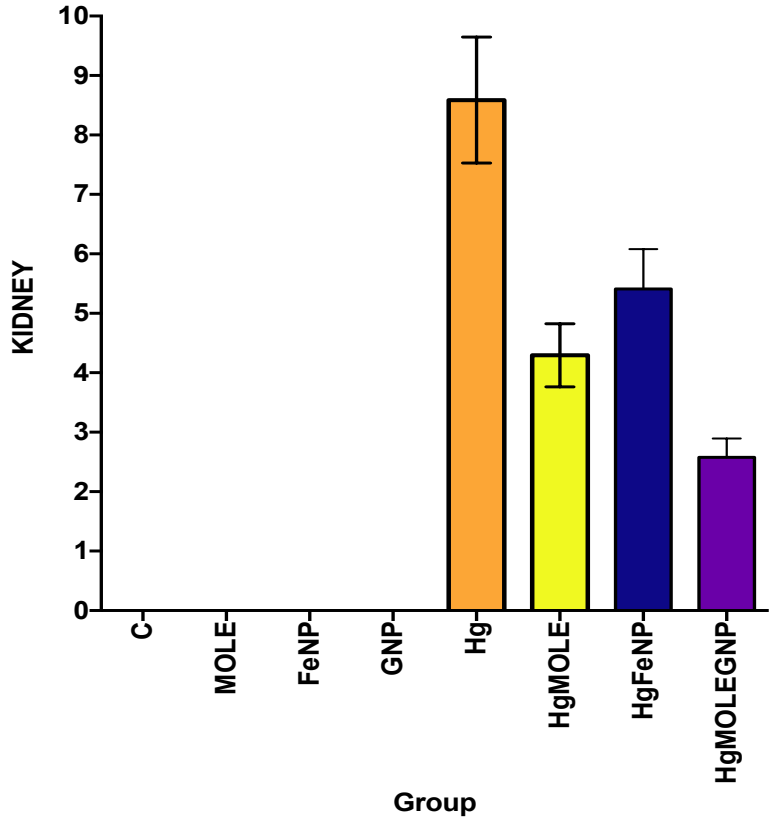

Figure7: mercury deposit in kidney

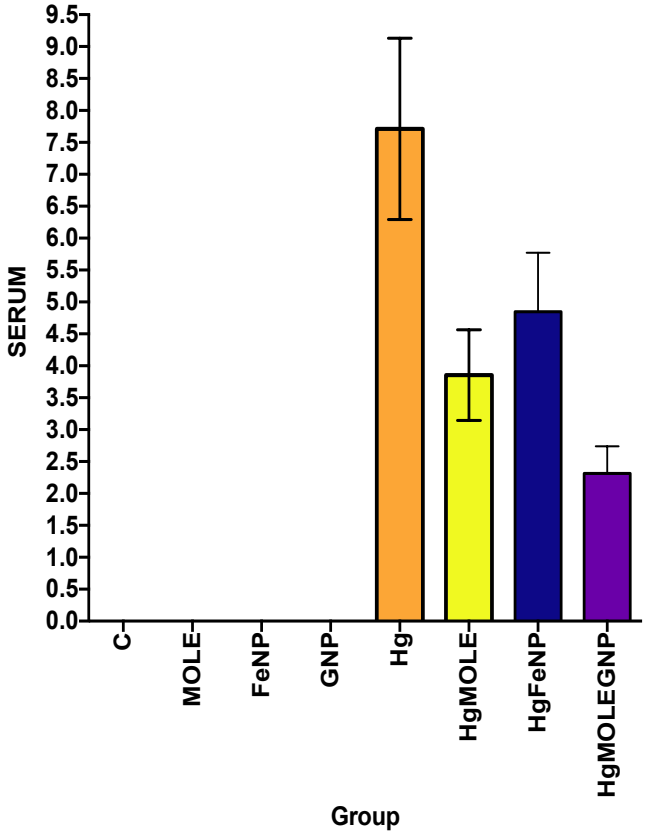

Figure 8. Mercury deposit in the serum

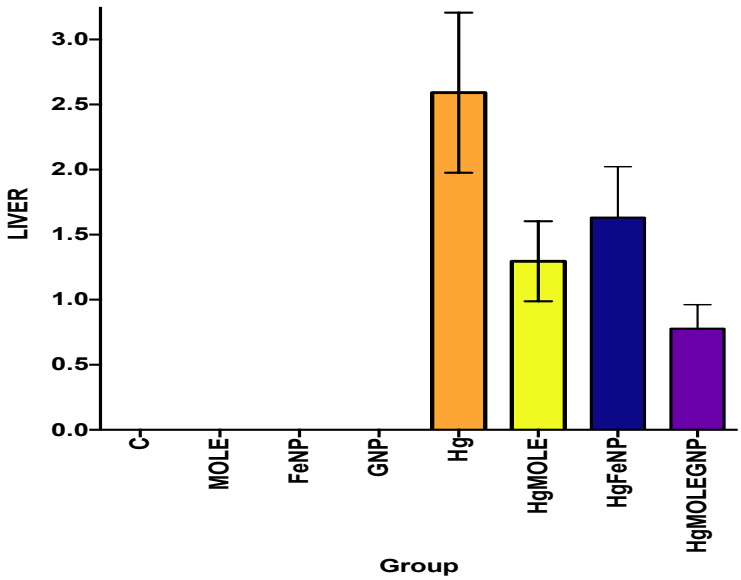

Figure 9. Mercury deposit in liver

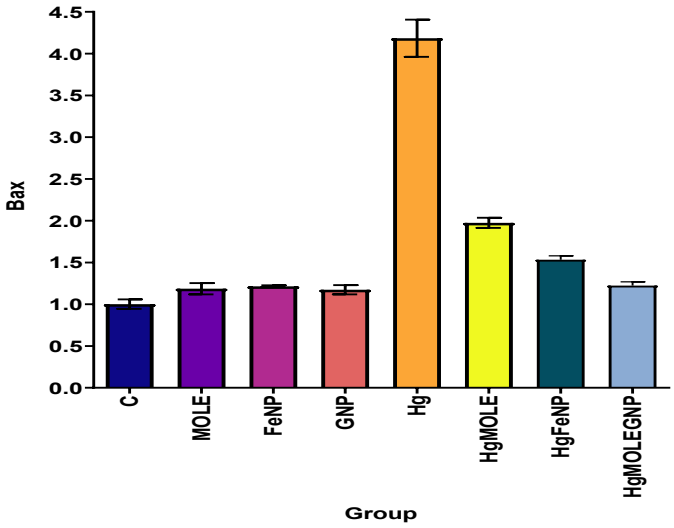

Figure 10: Bax gene expression

Table 1: **Oxidative stress**

	Control	MOLE	FeNP	MOLE-FeNP	Hg	Hg-MOLE	Hg-FeNP	Hg-MOLE-FeNP
MDA (uM)	1.792 ±	4.193 ±	3.875 ±	3.721±	6.867±	3.306±	3.406±	2.612±
	0.219	0.420	0.420	0.283	0.491	0.313	0.264	0.281
SOD (U/mL)	2.722 ±	1.076 ±	1.117 ±	1.111±	0.762±	1.461±	1.517±	2.051±
	0.411	0.148	0.111	0.092	0.076	0.201	0.151	0.313
CATALASE(umol/ml/mins)	7.904 ±	4.795 ±	5.022 ±	4.893±	3.805±	5.187±	5.433±	6.418±

	0.560	0.551	0.316	0.300	0.239	0.597	0.341	0.395
GSH (mM)	0.344 ±	0.185 ±	0.185 ±	0.189±	0.052±	0.181±	0.202±	0.241±
	0.038	0.019	0.016	0.023	0.022	0.050	0.019	0.013
GPX (U/L)	88.87 0±	64.54 3±	63.52 4±	65.465±	46.102	68.231 ±	67.154 ±	78.817±
	12.06 4	4.147	6.074	4.416	2.962	4.384	6.421	5.605
TAC (mM/g tissue)	1.135 ±	0.605 ±	0.610 ±	0.639±	0.336±	0.643±	0.674±	0.771±
	0.022	0.042	0.020	0.040	0.024	0.021	0.043	0.046
LDH (U/L)	45.54 6±	71.94 3±	70.09 1±	70.579±	189.32 4±	75.624 ±	76.151 ±	57.488±
	7.745	4.128	0.586	2.749	10.864	0.632	2.966	6.562

4.0 DISCUSSION

The results of the study show that heavy metals including mercury induce toxicity in animal tissues and serum by generating reactive free radicals that can lead to cellular damage, damage to lipid bilayer and DNA thereby degenerating to oxidative stress. The result of this work was in accordance with the work of Danaei *et al.*, (2018) which asserts that mercury poisoning causes damage to organs and tissues. The activities of Malondialdehyde (MDA) and **Lactic acid dehydrogenase (LDH) catalysizes** increased by 282.9% and 315.5% respectively after the administration of mercury, while the activities of other natural occurring antioxidant enzymes decreased its activities as follow CAT (51.9%), GPx (88.87%), GSH (84.o%), TAC (70.3%) and SOD (72.00%) respectively. However, after the administration of green nanoparticle, the activities of antioxidant enzymes was reversed to almost what it was in the positive control group with the corresponding decrease in the activities of MDA and LSH respectively as shown in table 1 above. The results also affirm the assertion of Karade *et al*., (2019), which assert that exposure of biological system to mercury leads to oxidative stress. The study revealed that chronic exposure of adult male rats to mercury leads to mercury deposit in the tissues of kidney, liver, and serum respectively as indicated in figures 7, 8, and 9 above. The figures7, 8 And 9 above went further to infer that there was no presence of mercury in those tissues and serum prior to the introduction of mercury. However the administration of MOLE, FeO-NPs, and MOLE-FeO-NPs, respectively on mercury induced rats decreases the activities of mercury, indicating that the three solutions have the capacity to ameliorate the effect of mercury in the biological system with MOLE- FeO-NPs having the greatest ameliorative effect. This was supported by the reported of Zeng *et al.,*(2019), and Mansour *et al.* (2014), which demonstrated renal protecting effects of MOLE against heavy metal toxicity via regulation of renal functions and prevention of oxidative damage as well as inflammatory reactions. There was an increase in the transcriptional level of apoptosis related Bax gene in Mercury poisoned rat as shown in figure 10 above. It was observed that the transcriptional level of apoptosis related Bax gene expression was at the minimal level before the administration of mercury. However, with the introduction of mercury, skyrocketed the transcriptional level showing that mercury can induce transcription of apoptosis related gene Bax. Nevertheless, administrations of MOLE, FeNPs and MOLE-FeNPs showed significant amelioration in the toxic effect of Hg. With MOLE-FeNP, showing the greatest effect indicating that green iron nanoparticles has a greater potentials of reducing mercury effect on biological system.

5.0 CONCLUSION

This study shows that exposure of the biological system and organs such as livers, kidneys, and serum to heavy metals such as mercury cause adverse effect by reducing their functionality and may result to oxidative stress and organ damage. However, the administration of MOLE, FeNP and MOLE-FeNP, have shown a significant reduction in mercury effect in those organs with MOLE-FeNP proven to be most effective in ameliorating Hg toxin. Therefore green synthesized iron oxide nanoparticles ameliorate the oxidative stress and Bax gene expression induced by mercury.

5.2. RECOMMENDATION

Based on the result of the research carried out, it has been proven that green synthesized iron nanoparticles can effective ameliorate the effect of mercury induced toxins however, further research is recommended and in the areas of histopathology and immunohistochemical studies to ascertain the level of damage of mercury on the morphology of those organs, tissues and immune system, and also further establish the ameliorative potentials of the green synthesized iron nanoparticles.

REFERENCES

Abd-Elhakim, Y.M, El Bohi, K. M, Hassan, S. K, El Sayed, S, Abd-Elmotal, S. M, (2018). Palliative effects of Moringa olifera ethanolic extract on hemato-immunologic impacts of melamine in rats. *Food Chem. Toxicol.* 114, 1–10.

Abdull Razis, A.F, Ibrahim, M.D, Kntayya, S.B., (2014). Health benefits of Moringa oleifera. Asian Pac. *J. Cancer Prev.* 15, 8571–8576.

Abou-Zeid, S.M, Ahmed, A.I, Awad, A, Mohammed, W.A, Metwally, M, Almeer, R, Abdel- Daim, M.M, Khalil, S.R, (2021). Moringa oleifera ethanolic extract attenuates tilmicosin-induced renal damage in male rats via suppression of oxidative stress, inflammatory injury, and intermediate filament proteins mRNA expression. Biomed. Pharmacother. = Biomed. Pharmacother. 133, 110997.

Adil, S. F, Assal, M. E, Khan, M, Al-Warthan, A, Siddiqui, M. R, Liz-Marz´ an, L.M, (2015). Biogenic synthesis of metallic nanoparticles and prospects toward green chemistry.

Aja, P, (2014). Chemical constituents of Moringa oleifera leaves and seeds from Abakaliki, Nigeria. Am. J. Phytomed. Clin. Ther. 2, 310–321.

Aja, P, *et al*, (2015). Evaluation of anti-diabetic effect and liver function indices of ethanol extracts of Moringa oleifera and Cajanus cajan leaves in alloxan induced diabetic albino rats. *Glob. Vet.* 14, 439–447.

Anwar, F., Latif, S., Ashraf, M., Gilani, A.H., (2007). Moringa oleifera: a food plant with multiple medicinal uses. Phytother. Res.: Int. J. Devoted Pharmacol. *Toxicol. Eval. Nat. Prod. Deriv*. 21, 17–25.

Bhattacharya, A., Tiwari, P., Sahu, P.K., Kumar, S, (2018). A review of the phytochemical and pharmacological characteristics of Moringa oleifera. *J. Pharm. Bioallied Sci*. 10, 181–191.

Castoldi A. F, Coccini T, Manzo L.(2003). Neurotoxic and molecular effects of methylmercury in humans. *Rev Environ Health.* ;18(1):19-31.

Chatterjee, A., Mridha, D., Banerjee, J., Chanda, S., Ray, K., Acharya, K., Das, M., Roychowdhury, T. and Sarkar, J. (2021). Green synthesis of iron oxide nanoparticles and their ameliorative effect on arsenic stress relief in Oryza sativa seedlings. Biocatalysis and Agricultural Biotechnology 38:102207.

Danaei, M., Dehghankhold, M., Ataei, S., HasanzadehDavarani, F., Javanmard, R., Dokhani, A., Khorasani, S. and Mozafari, M. (2018). Impact of particle size and polydispersity index on the clinical applications of lipidicnanocarrier systems. *Pharmaceutics* 10 (2):57.

Davinelli, S., Bertoglio, J.C., Zarrelli, A., Pina, R., Scapagnini, G., (2015). A randomized clinical trial evaluating the efficacy of an anthocyanin–maqui berry extract (Delphinol®) on oxidative stress biomarkers. *J. Am. Coll. Nutr.* 34, 28–33.

Devi, H.S., Boda, M.A., Shah, M.A., Parveen, S. and Wani, A.H. (2019). Green synthesis of iron oxide nanoparticles using Platanusorientalis leaf extract for antifungal activity. Green Processing and Synthesis 8 (1):38-45.

Dobson, R.L., Motlagh, S., Quijano, M., Cambron, R.T., Baker, T.R., Pullen, A.M., Regg, B. T., Bigalow-Kern, A.S., Vennard, T., Fix, A., Reimschuessel, R., Overmann, G., Shan, Y., Daston, G.P., (2008). Identification and characterization of toxicity of contaminants in pet food leading to an outbreak of renal toxicity in cats and dogs. *Toxicol. Sci.* 106, 251–262.

Duruibe JO, Ogwuegbu MOC, Egwurugwu JN. Heavy metal pollution and human biotoxic effects. International Journal of physical sciences. 2007;2(5):112-118

Ekor, M., (2014). The growing use of herbal medicines: issues relating to adverse reactions and challenges in monitoring safety. *Front. Pharmacol. 4, 177*

El-Hadary, A.E., Ramadan, M.F., (2019). Antioxidant traits and protective impact of Moringa oleifera leaf extract against diclofenac sodium-induced liver toxicity in rats. *J. Food Biochem.* 43, 12704.

El Shanawany, E.E., Fouad, E.A., Keshta, H.G., Hassan, S.E., Hegazi, A.G., AbdelRahman, E.H., (2019). Immunomodulatory effects of Moringa oleifera leaves aqueous extract in sheep naturally co-infected with Fasciola gigantica and Clostridium novyi. *J. Parasit. Dis.* 43, 583–591.

Fauad.D.E, Zhang C.H, Didamany H, Lui Y, Fadele D.M, Shah A.H,(2019). Improved size, morphology and crystallinity of hematite (α-Fe_2O_3) nanoparticles synthesized via the precipitation route using ferric sulfate precursor. *ScienceDirect vol 12. 1253 - 1261*

Hammond,C.R(2005).The Elements (http://www-d0.fnal.gov/hardware/cal/lvps_info/engine) Archived(https://web.archive.org/web/20080626181434/http://wwwd0.fnal.gov/hardware/cal/lvp s_inf) . CRC Handbook of Chemistry and Physics (86th ed.). Boca Raton (FL): CRC Press. ISBN 0-8493-0486-5.

Helal, F, and El- Mokhtar M.A, (2018). Effect of dietary moringa (Moringa oleifera) and rosemary (Rosmarinus officinalis) leaves or their mixture on productive performance, carcass characteristics and antioxidant enzymes of rabbits reared under heat stress conditions. CIGR J. 19, 184–192.

Karade V.C, Parit S.B, Dawkar V.V, Daven R.S, Choudhary R.J, Kedge V.V,(2019). A green approach for the synthesis of α-FeO_3 nanoparticlles from gardenia resinifere plant

and it's in vitro hyperthermia application. Elsevier 2405- 8440

Karthivashan, G. (2015). The molecular mechanism underlying the hepatoprotective potential of Moringa oleifera leaves extract against acetaminophen induced hepatotoxicity in mice. J. Funct. Foods 17, 115–126.

Khalil S.R, Abdel-Matal S.M, Abd-Elsalam.M, El-Hameed N. E. A, and Award A,(2020). Retoring Strategy of ethanolic extract of moringa oleifera leave against tilmicosin-induced cardiac injury in rats targeting cell apoptosis-mediated pathways. ScienceDirect Gene vol 730 144-272.

Khan, M., Shaik, M.R., Adil, S.F., Khan, S.T., Al-Warthan, A., Siddiqui, M., Tahir, M.N., Tremel, W., (2018). Plant extracts as green reductants for the synthesis of silver nanoparticles: lessons from chemical synthesis. Dalton Trans. 47, 11988–12010.

Khan, M., Shaik, M. R., Adil, S.F., Khan, S.T., Al-Warthan, A., Siddiqui, M., Tahir, M.N., Tremel, W. (2018). Plant extracts as green reductants for the synthesis of silver nanoparticles: lessons from chemical synthesis. Dalton Trans. 47, 11988–12010.

Madhavi V, Prasad T.N.V.K.V, Reddy A.V.B, Ravindra Reddy B, and Madhavi G,(2013) "Application of phytogenic zero valent iron nanoparticles in the adsorption of hexavalent chromium," Spectrochimica Acta A: Molecular and Biomolecular Spectroscopy,vol.116,pp.17–25,2013.

Mansour, H.H.(2014). Protective effect of Moringa oleifera on γ-radiation-induced hepatotoxicity and nephrotoxicity in rats. Am. J. Phytomed. Clin. Ther. 2, 495–508.

Mansour, M., Arisha, A., AlGamal, M., Elsayed, A., Saad, S., El Bohi, K., (2020). Effect of Moringa oleifera leaves extract-SeNPs conjugate administration on testicular toxicity induced by melamine in rats. Zagazig Vet. J. 48, 213–227.

Narayanan S, Sathy B.N, Mony U, Koyakutty M, Nair S.V, and Menon D,(2012). "Biocompatible magnetite /gold nanohybrid contrast agents via green chemistry for MRI and CT bioimaging," ACS AppliedMaterialsandInterfaces,vol.4,no.1,pp. 251–260,2012

Njagi E.C, Huang,H, Staffordetal L,(2011)."Biosynthesis of iron and silver nanoparticles at room temperature using aqueous sorghum bran extracts,"Langmuir,vol.27,no.1,pp.264–271.

Obembe, O.O., Raji, Y.J.A., 2018. Effects of aqueous extract of Moringa oleifera seed on cadmium-induced reproductive toxicity in male Wistar rats. Afr. Health Sci. 18, 653–663.

Santos, C.S., Sotillo, A., Gupta, T., Delgado, S., Müller, W., Stienen, E.W., de Neve, L., Lens, L., Soares, A.M. and Monteiro, M.S. (2020). Mercury Uptake Affects the Development of Larusfuscus Chicks. Environmental Toxicology and Chemistry 39 (10):2008-2017.

Santos, C.S.A., Blondel, L., Sotillo, A., Müller, W., Stienen, E.W.M., Boeckx, P., Soares, A.M.V.M., Monteiro, M.S., Loureiro, S., de Neve, L. and Lens, L. (2017). Offspring Hg exposure relates to parental feeding strategies in a generalist bird with strong individual foraging specialization. Science of The Total Environment 601-602:1315-1323.

Shahwan T, Abu S, Sirriah M. Nairat L,(2011). "Green synthesis of iron nanoparticles and their application as a Fenton-like catalyst for the degradation of aqueous cationic and anionic dyes,"*Chemical Engineering Journal,vol.172,no.1,pp.258–266,.*

Sreelatha, S., Padma, P., (2009). Antioxidant activity and total phenolic content of Moringa oleifera leaves in two stages of maturity. Plant Foods Hum. Nutr. 64, 303–311.

Venkateswarlu Rao S.Y.S, Balaji T, Prathima B, and Jyothi N.V.V,(2013)."Biogenic synthesis of Fe3O4 magnetic nanoparticles using plantain peel extract,"MaterialsLetters,vol.100,pp.241–244.

Vergara-Jimenez, M., Almatrafi, M.M., Fernandez, M.L., (2017). Bioactive components in Moringa oleifera leaves protect against chronic disease. Antioxidants 6, 91. Vogt, M., Bauer, M.K., Ferrari, D., Schulze-Osthoff, K., 1998. Oxidative stress and hypoxia/reoxygenation trigger CD95 (APO-1/Fas) ligand expression in microglial cells. FEBS Lett. 429, 67–72.

Zeng, K., Li, Y., Yang, W., Ge, Y., Xu, L., Ren, T., Zhang, H., Zhuo, R., Peng, L., Chen, C., Zhou, Y., Zhao, Y., Li, W.J., Jin, X., Yang, L., 2019. Moringa oleifera seed extract protects against brain damage in both the acute and delayed stages of ischemic stroke. Exp. Gerontol. 122, 99–108.

Zhang, X.-H., Zhang, X., Wang, X.-C., Jin, L.-F., Yang, Z.-P., Jiang, C.-X., Chen, Q., Ren, X.-B., Cao, J.-Z. and Wang, Q. (2011). Chronic occupational exposure to hexavalent chromium causes DNA damage in electroplating workers. *BMC Public Health* 11 (1):1-8.